VPS VIBRATIONS IN PHYSICAL SYSTEMS

DOI: 10.21008/j.0860-6897.2022.2.18
Vibrations in Physical Systems, 2022, 33(2), 2022218

Measurement of the Surface Reflectance of an Acoustic Wave Using Wave Packets Propagating in a Circular Waveguide

Piotr WRZECIONO, Michał SZYMAŃSKI

Institute of Information Technology – SGGW, Nowoursynowska 159, Warszawa,

Corresponding author: Piotr WRZECIONO, email: piotr_wrzeciono@sggw.edu.pl

Abstract The main idea of the measurement presented in this paper was to separate the incident wave from the reflected wave. For this purpose, short wave packets and a sufficiently long waveguide with a circular cross-section were used. Several types of wave packets were developed and used in the experiment. We found that a wave packet of 5 ms duration could be propagated in a waveguide of length 5.6 meters without significant sound level losses. We used an audio interface operating at a sampling rate of 96 kHz in the measurements. The limit of wave propagation without dispersion phenomenon was determined. The developed measurement methodology made it possible to maintain the same air temperature along the entire length of the tested waveguide since short pulses did not cause the speaker temperature to rise. Avoiding this effect reduced the measurement uncertainty of the reflection coefficient.

Keywords: wave packets, surface reflectance coefficient, dispersion, waveguide.

1. Introduction

Currently, several standards are related to measuring reflectance and sound absorption. Two of them [1,2] are related to measuring using the standing wave phenomenon in a pipe. The third method is related to building acoustics [3]. However, despite measurement standards, there is a relatively considerable measurement uncertainty [4,5]. This fact prompted us to look for more accurate measurement methods. Our inspiration came from reflectometric measurement methods in optical fibers.

Our method is similar to optical time-domain reflectometry (OTDR). So let's recall the basics of the latter [6-8]. OTDR has been established for analyzing reflectivities and losses in optical fibers according to the following scheme. First, a short light pulse is generated by a single-mode laser diode and injected into the tested optical fiber through a launch cable. Then, the reflected beam, extracted with a directional fiber coupler and collected by a fast and sensitive photodetector, becomes the subject of the analysis.

Two physical phenomena underlie OTDR. First, Fresnel reflection occurs at the interface between two transparent media with different refractive indices. In optical fibers, those places are at connectors, breaks, mechanical splices, or ends. Second, Rayleigh scattering is an effect of the interaction of electromagnetic waves with objects much smaller than the wavelength. In optical fibers, these objects are microscopic irregularities of the glass structure. Once the light pulse is injected into the tested fiber, the reflectometer sets a timer. At the input end, the dedicated analyzer records the power of the returned light versus time. The slope of the plot allows for assessing the propagation losses, while the sudden discontinuities are for localizing defects of a different type.

Transferring the OTDR methodology to acoustic applications required development and experiments related to various types of acoustic pulses. Our research focuses on the propagation of pulses in the waveguide, observation of the behavior of the sound source, and the dispersion phenomenon.

2. Acoustic experimental waveguide

The primary design consideration was the ability to generate pulses and observe their propagation. Thus, the essential design elements were a sound source: a loudspeaker, a circular pipe with smooth inner walls, and a system of two measurement microphones. We used a PVC pipe with an inner diameter of 110 mm and a length of 5.6 m. The waveguide [9] was constructed from five segments of 1 m length and one segment of 0.6 m length. We used rigid PVC pipes that did not vibrate during measurements. We mounted two ECM 8000 measurement microphones in the middle segment, with a distance of 0.6 m between the microphones. The sound source was a speaker mounted in a damped enclosure, controlled by a power amplifier and the U-PHORIA UMC1820 audio interface. The audio interface was configured to operate at a sampling rate of

96 kHz. We calibrated the audio system according to the sound level of 94 dB at a frequency of 1 kHz using the SONOPAN KA-50 calibrator. To measure the air temperature inside the waveguide, we used a UT58C universal meter. The figures (see Fig.1 and Fig.2) show the implementation of the experimental system. The microphone designations (see Fig. 2) are used throughout our experiments. Microphone no. 1 is closer to the sound source than microphone no. 2.

Figure 1. The experimental waveguide. The left side of the photo shows the speaker enclosure.

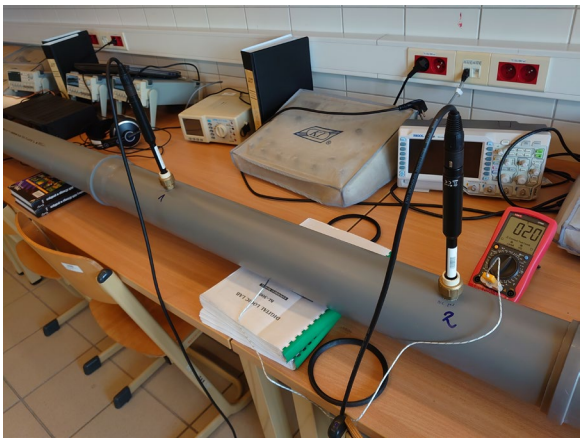

Figure 2. The arrangement of microphones. Microphone no. 1 is on the left side of the photo.

3. Wave packets

A wave packet is a short pulse of a specific duration [10]. By shaping the wave packet, it is possible to observe the behavior of broadband pulses, such as sinc(x) type, or narrowband pulses, such as sinusoidal pulses. In our experiment, we used pulses with a duration of 5 ms. During this time, the sound pulse travels a distance of about 1.72 meters (at 20°C). This value is comparable to the distance between microphone 2 (see Fig. 2) and the end of the waveguide. Thus, separation of the incident and reflected pulse is feasible without dispersion. We used wave packets described by formulas (1), (2), and as below:

$$x_1(t) = \Pi\left(\frac{t}{5ms}\right)\mathrm{sinc}\left(\frac{t-5ms}{5ms}\right), \tag{1}$$

$$x_2(t) = \Pi\left(\frac{t-5ms}{5ms}\right)\sin(2\pi f_0 t), \tag{2}$$

$$x_3(t) = \exp\left(\frac{-a^2\cdot t^2}{2T_s^2}\right)\sin(2\pi f_0 t), \tag{3}$$

where:

$$\mathrm{sinc}(x) = \begin{cases} \frac{\sin(x)}{x} \; for\; x \neq 0 \\ 1 \quad for x = 0 \end{cases}, \tag{4}$$

$$\Pi\left(\frac{t}{T}\right) = \begin{cases} 0\; for\; |t| > \frac{T}{2} \\ \frac{1}{2}\; for\; |t| = \frac{T}{2} \\ 1\; for\; |t| < \frac{T}{2} \end{cases} \tag{5}$$

Formula (1) describes an impulsive wave packet. Equation (2) defines a wave packet in a rectangular window (5). Next, formula (3) is a Gaussian wave packet. In formulas (1-3), and (5), the variable t represents time, and f_0 is the fundamental frequency. In formula (3), coefficient a is a positive constant that determines the width of the Gaussian function. Formula (4) describes the sinc function. Formula (5) defines the rectangle window, where T represents its duration. Finally, the quantity T_s in formula (3) is the sampling period of the digital signal.

Formulas (1-2) include a wave packet duration of 5 ms. This duration is sufficient time to separate the incident and reflected waves in our experiment. We created formulas (1-5) based on the literature on wave packets [10] and digital signal processing [11].

All pulses were generated using the Octave program. Wave packet (3) used the default value of a, which is 2.5. We used standard acoustic thirds frequencies to test windows (2-3). Each of the above defined wave packets: (1-3) were tested to see which of them allows separation of the incident and reflected pulse.

Using two microphones placed relatively far from each other (60 cm), we could check what type of wave propagated in the waveguide. Controlling the type of wave is very important because, for a correct measurement, it is necessary to be sure that the wave is flat [1, 2] and the transmission is single-mode.

4. Wave packet test results

During testing, the waveguide was closed with a PVC plug. The plug had a mass of 0.068 kg, while the density of the PVC was 1450 kg/m^3. The pulsed wave packet (1) provided inconclusive results. As critical problems we can specify capturing the beginning of the pulse and significant difference between the waveform and original signal (see Fig. 3).

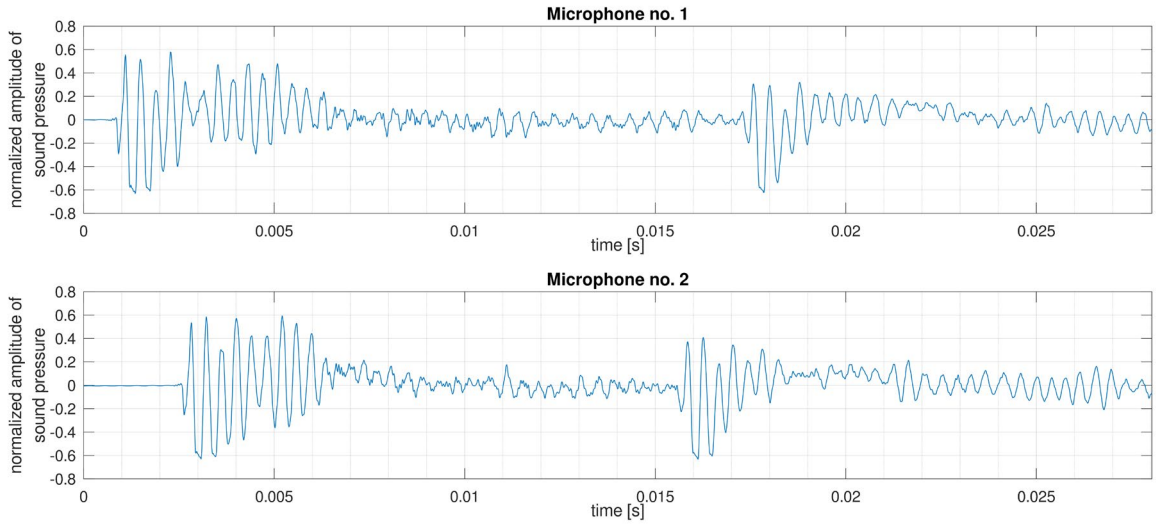

Figure 3. Propagation of an impulsive wave packet. The upper waveform is from microphone no. 1, and the lower is from microphone no. 2. The figure shows the incident wave and one reflection from the end of the waveguide.

The result was already qualitatively better for the wave packet (2). However, the harmonic distortion introduced into the system by the speaker is visible (see Fig. 4). The incident pulse (the first) is separated from the reflected one (second). Both are almost identical.

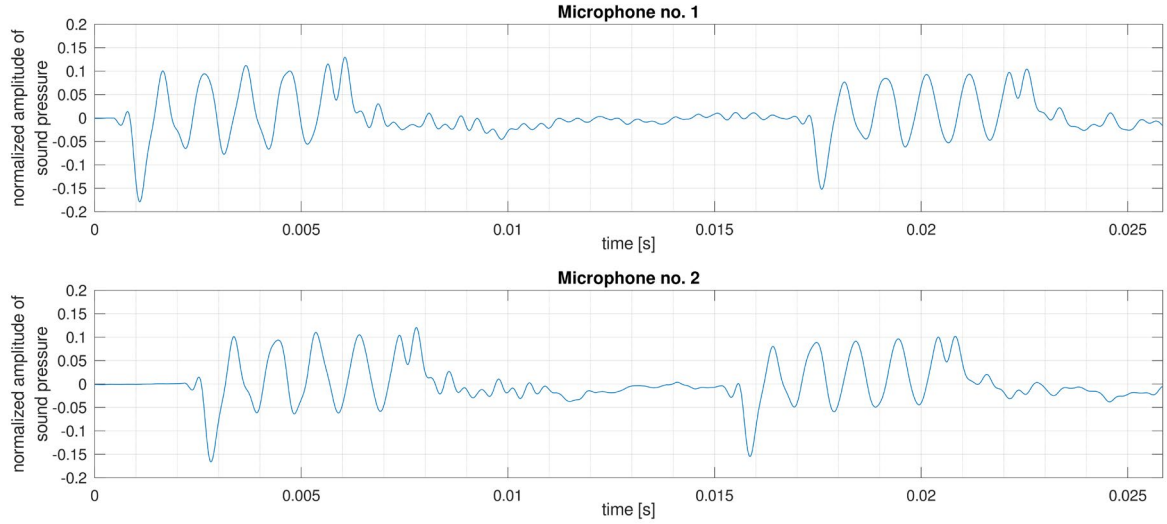

Figure 4. Propagation of a sinusoidal wave packet for f_0 = 1 kHz. The upper waveform is from microphone 1, and the lower is from microphone no. 2. The figure shows the incident wave and one reflection from the end of the waveguide.

In a wave packet with a Gauss envelope (3), the signal differs a little from the original (in the absence of dispersion). This phenomenon occurs because the incident and reflected pulses are separated. However, the mechanical inertia of the speaker diaphragm is also noticeable (see Fig. 5).

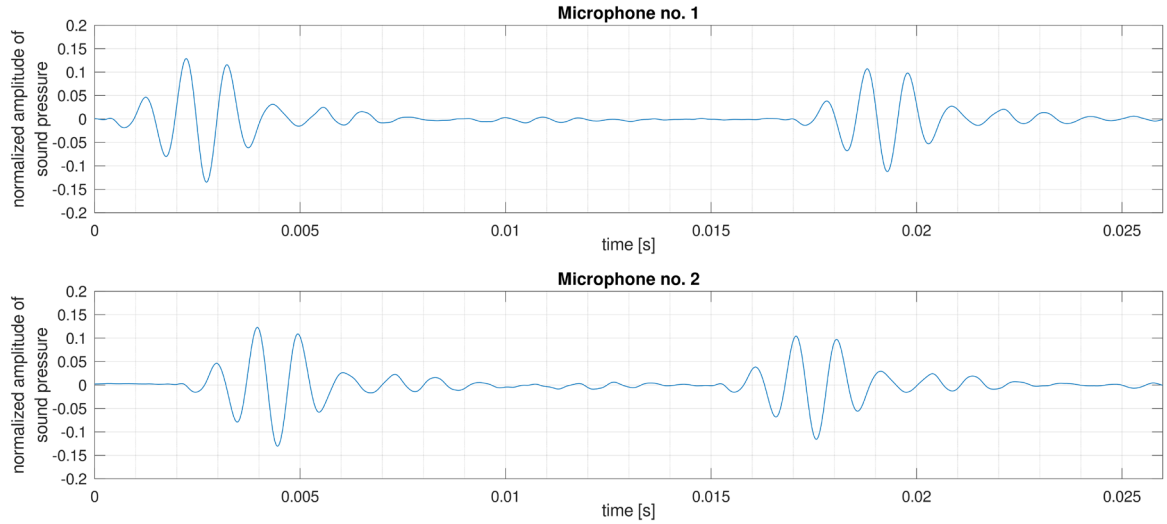

Figure 5. Propagation of a Gaussian wave packet for f_0 = 1 kHz. The upper waveform is from microphone no. 1, and the lower from microphone 2. The figure shows the incident wave and one reflection from the end of the waveguide.

In the tested system, the sent pulse repeatedly bounced off the end of the waveguide and off the speaker. In single-mode transmission, the individual wave packets are separated from each other. However, dispersion impedes separation when the wavelength associated with the transmitted wave packet allows subsequent modes [11,12] to excite (see Fig. 6).

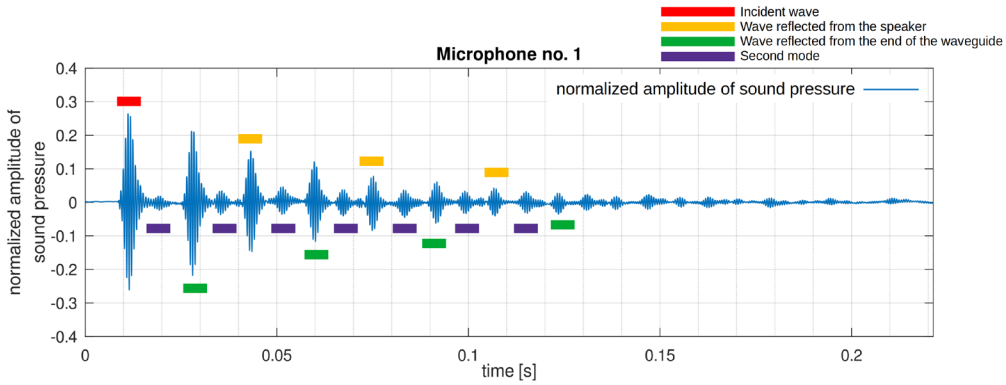

Figure 6. Propagation of a Gaussian wave packet with f_0 = 1600 Hz. The corresponding colors mark the incident pulse, the reflected pulses, and the wandering second mode pulse.

In addition, in the case of significant dispersion, we noticed an increase in the temperature of the speaker control amplifier enclosure, from 20°C (ambient temperature) to 35°C.

5. Reflectance measurement

After conducting measurement tests of the waveguide, we calculated the reflection coefficient only when we could separate the individual wave packets. This phenomenon occurs when a single mode is propagated, or we could split the wave packets of an individual wave from each other. After testing the wave packets, we chose the Gaussian type (3). This pulse is well reproduced by the speaker, unlike the other two (1) and (2). To determine the reflection coefficient R, we used the relationship between the energy of the incident and the reflected pulse (6):

$$R = \frac{E_R}{E_I}, \tag{6}$$

where R is the reflection coefficient, E_I is the energy of the incident wave packet, E_R represents the energy of the reflected packet. For a wave packet, represented in discrete form by a sequence of N samples, the energy is expressed by (7):

$$E = \sum_{k=0}^{N-1} |f(k)|^2 = \sum_{k=0}^{N-1} |f(kT_s)|^2. \tag{7}$$

In formula (7), N is the number of samples, $f(k)$ is the discrete signal, and T_s is the sampling period of the signal. The letter E represents energy. In the absence of dispersion, the length of the incident wave packet and the reflected wave packet are the same. Otherwise both wave packets are elongated. Thus dispersion increases the measurement uncertainty and hinders or even makes impossible separation of two wave packets. Using formulas (6) and (7), we calculate the reflection coefficient as (8):

$$R = \frac{E_R}{E_I} = \frac{\sum_{k=0}^{N-1} |f_R(k)|^2}{\sum_{k=0}^{N-1} |f_I(k)|^2}, \tag{8}$$

where $f_I(k)$ denotes the incident wave packet, and $f_R(k)$ is the reflected one.

The R factor defined in formulas (6) and (8) neglects the phase changes that occur during reflection. The purpose of this paper was to present the main principles of measuring the reflection coefficient using wave packets. Consideration of phase changes is planned for further research.

Due to the presence of multiple reflections of the wave packet, we can estimate the measurement uncertainty for the R factor. For this purpose, we used two methods. First, we evaluated the spread of energy values of individual wave packets by assessing the change in sound level at different values of N. The second method involved comparing the values of the R factor determined separately for microphone no. 1 and microphone no. 2.

For a sampling frequency of 96 kHz and single-mode transmission, the differences obtained when increasing or decreasing the number of samples by one did not exceed 0.03 dB. The number of samples of a 5 ms wave packet at the f_s=96 kHz is 480. Changing the sampling frequency to 48 kHz increased the tested uncertainty to 0.1 dB. Thus, the higher the sampling frequency, the smaller the error in estimating the sound level of the wave packet. The calculation of the described differences was defined by formula (9):

$$e_{rng} = \left|10\log_{10}\left(\frac{E_{RN}}{E_{RN+1}}\right)\right|, \tag{9}$$

where e_{rng} [dB] is the difference between the reflected signal energy calculated for a window of length N and the reflected signal energy calculated for a window of length $N+1$. E_{RN} represents the reflected wave energy calculated for a window of length N, and E_{RN+1} is the reflected wave energy for a window of size $N+1$.

For the second method of determining the measurement uncertainty, the arithmetic mean of the two R factors for microphone no. 1 and no. 2 measured for a given wave packet was used. The standard deviation of the determined coefficients was chosen as the relative measurement uncertainty. The mentioned above method of calculating measurement uncertainty is described by formula (10):

$$\begin{aligned} R_{AV} &= \frac{R_1+R_2}{2} \\ e_{r12} &= \frac{100}{\sqrt{2}R_{AV}}\sqrt{(R_{AV}-R_1)^2+(R_{AV}-R_2)^2}, \end{aligned} \tag{10}$$

where R_1 is the reflection coefficient calculated for microphone no. 1, R_2 is the reflection coefficient calculated for microphone no. 2, e_{r12} is the relative measurement uncertainty of calculating R using both microphones, expressed as a percentage.

Reflectance measurements were carried out for frequencies of musical thirds [9]. However, due to multimodality, we presented the results only for the separable wave packets (Table 1).

Table 1. Results of R calculation.

Frequency [Hz]	R - Microphone no. 1	R - Microphone no. 2	Average R	Uncertainty [%]
200	0.86	0.94	0.90	4.72
250	0.88	0.98	0.93	5.52
315	0.85	0.92	0.88	3.57
400	0.85	0.86	0.85	0.81
500	0.78	0.77	0.78	0.46
630	0.695	0.698	0.70	0.23
800	0.64	0.67	0.65	2.65
1000	0.70	0.78	0.74	4.95
1250	0.74	0.72	0.73	1.15
1600	0.67	0.73	0.70	4.14
2000	0.85	0.68	0.76	11.46

The values of the coefficients obtained separately for microphones no. 1 and no. 2 differ a little from each other. However, a significant increase in the spread of values appears with the appearance of the second mode. The graph (see Fig. 7) presents the obtained results.

During the measurements, we observed the vibrations of our chosen waveguide closure plug. The consequence of this phenomenon is a reduction in the value of the reflection coefficient R (see Table 1).

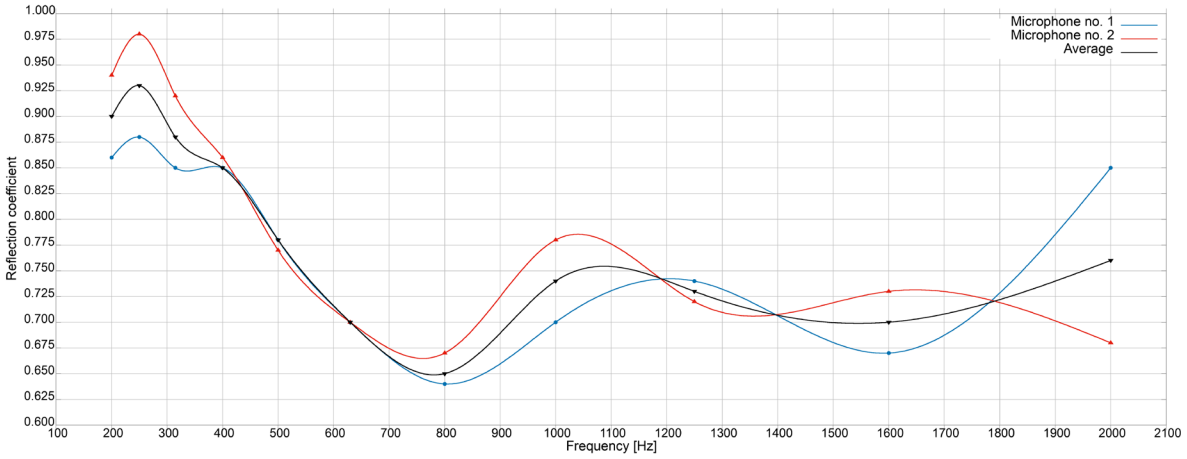

Figure 7. The graph of the measured reflection coefficient R for a closed waveguide.

6. Discussion

While conducting experiments with the described measurement system, we observed several problems that affect the overall quality of the measurement. The first was the inaccurate generation of the desired pulse, as shown in the figures (see Figs 1-2). The speaker membrane vibrated even after the pulse ended. Minimizing this phenomenon can be achieved by increasing the amplifier's damping factor [9]. Thus, to improve sound generation by the speaker, the power amplifier's quality must also be considered.

The second phenomenon was the amplifier's power transistors temperature rise while a strong pulse dispersion occurs. This effect is a consequence of electrical current generation by the speaker coil moved by the vibrating diaphragm and can cause an increase of measurement uncertainty for the described system. Therefore, a power amplifier with higher damping factor should be recommended [9].

When additional modes in the waveguide appear, the difference between the R coefficients obtained from the two microphones increases. Therefore, for single-mode transmission, the mentioned differences require further study.

The above mentioned issues can also affect the measurement uncertainty of the methods described in standards [1,2] and other works using waveguides [12,13]. However, the standards themselves [1,2] do not mention changes in the thermal conditions of the loudspeaker as a factor that worsens measurement uncertainty since the temperature of the air near the loudspeaker may increase during the measurement. Consequently, in pipes described in the standards [1, 2], inhomogeneous temperature distributions may appear causing, in turn, local speed of sound variations inside the waveguide [9].

Using short wave packets under single-mode transmission conditions does not change the temperature inside the waveguide, as we observed when conducting the experiments. Thus, compared to other methods [1-3,9,12-13], the measurement uncertainty obtained should be better or comparable. The minimum measurement error obtained in our experiment is 0.2%. For a few selected frequencies, it is about 5%. The measurement error obtained in methods using waveguides [12,13] was about 3.7%. In comparison, the measurement uncertainty of the method used in building acoustics [3] is estimated at 30% [4,5]. As for the measurement error of the methods described in the standards [1,2] is observed as discrepancies in measurement results obtained in different laboratories [5,12,13]. The variety of results can be as wide as 20% [5]. However, it is not clear why the difference is so significant. In conclusion, the measurement uncertainty of the method we presented is at least as small as in other methods using waveguides [12,13]. However, a prerequisite for the good performance of our system is the single-mode transmission.

Timing accuracy is important in measurements using wave packets [6-8]. Our system uses digital signals and thus depends primarily on the sampling frequency. The fundamental condition is the Nyquist sampling theorem [9]. However, the higher the sampling frequency, the lower the measurement uncertainty.

7. Conclusion

The method of measuring the reflection coefficient using wave packets presented in this paper enables the effective separation of the incident and reflected wave. In the case of single-mode transmission, a measurement uncertainty of about 0.5% can be obtained, which is small compared to other methods, especially the results obtained according to the standard designed for building acoustics. Furthermore, the

observed thermal phenomena associated with the speaker's work can be considered during different reflectance or absorption measurements to minimize the measurement uncertainty. In further work, we plan to take into account the phase shift and analyze the propagation of the wave packet when multiple modes exist. Future work will also involve the development of an acoustically suitable rigid plug for the waveguide, which will have a reflection coefficient R close to unity for the entire measurement bandwidth.

Additional information

The authors declare: no competing financial interests and that all material taken from other sources (including their own published works) is clearly cited and that appropriate permits are obtained.

References

1. PN-EN ISO 10534-1:2004; Akustyka. Określanie współczynnika pochłaniania dźwięku i impedancji akustycznej w rurach impedancyjnych. Część 1: Metoda wykorzystująca współczynnik fal stojących.
2. PN-EN ISO 10534-2:2003; Akustyka. Określanie współczynnika pochłaniania dźwięku i impedancji akustycznej w rurach impedancyjnych. Część 2: Metoda funkcji przejścia.
3. PN-EN ISO 354:2005; Akustyka. Pomiar pochłaniania dźwięku w komorze pogłosowej.
4. A. Iżewska, K. Czyżewski; Niepewność pomiaru współczynnika pochłaniania dźwięku w komorze pogłosowej (in Polish); Prace Instytutu Techniki Budowlanej 2011, 40, 3-13.
5. F. Orduna-Bustamante, F. Arturo Machuca-Tzili, R. Velasco-Segura; Evaluation of the bias error of transmission tube measurements of normal-incidence sound transmission loss using narrow tube reference elements; J. Acoust. Soc. Am. 2018, 144(2), 1040-1048. DOI:10.1121/1.5051649
6. M.K. Barnoski, S.M. Jensen; Fiber waveguides: a novel technique for investigating attenuation characteristics; Appl. Optics 1976, 15(9), 2112-2115. DOI: 10.1364/AO.15.002112
7. J.P. Dakin, R.G.W. Brown; Handbook of Optoelectronics: Concepts, Devices, and Techniques (Volume One), Taylor & Francis (CRC Press), 2020.
8. A. H. Hartog; An introduction to distributed optical fibre sensors; Taylor & Francis (CRC Press), 2017.
9. F.A. Everest, K.C. Pohlmann; Master handbook of acoustics; McGraw-Hill Education, 2022.
10. F. Arickx, J. Broeckhove, W. Coene, P. Van Leuven; Gaussian wave-packet dynamics; Int. J. Quantum Chem. 1986, 30(S20), 471- 481. DOI: 10.1002/qua.560300741
11. B.P. Lathi; Linear Systems and Signals, 2nd Edition; Oxford University Press, 2004.
12. J. Prisutova, K. Horoshenkov, J.-P. Groby, B. Brouard; A method to determine the acoustic reflection and absorption coefficients of porous media by using modal dispersion in a waveguide; J. Acoust. Soc. Am. 2014, 136(6), 2947-2958. DOI: 10.1121/1.4900598
13. W. Duan, R. Kirby, J. Prisutova, K.V. Horoshenkov; Measurement of complex acoustic intensity in an acoustic waveguide; J. Acoust. Soc. Am. 2013, 134(5), 3674-3685. DOI: 10.1121/1.4821214